Sustainable Cities and Society 96 (2023) 104695

Contents lists available at ScienceDirect

Sustainable Cities and Society

journal homepage: www.elsevier.com/locate/scs

How does the visual environment influence pedestrian physiological stress? Evidence from high-density cities using ambulatory technology and spatial machine learning

Meng Cai [a,b,1], Luyao Xiang [c,*,1], Edward Ng [b,c]

[a] School of Urban Design, Wuhan University, Wuhan, 430072, PR China
[b] Institute of Future Cities, The Chinese University of Hong Kong, Hong Kong
[c] School of Architecture, The Chinese University of Hong Kong, Hong Kong

ARTICLE INFO

Keywords:
Skin conductance level
Ambulatory technology
Street view
Isovist
Geographical random forest
Moving window

ABSTRACT

Revealing the phased impacts of the visual environment on physiological stress in outdoor environments can facilitate accurate and practical planning strategies towards healthy and sustainable living environments. This study adopted ambulatory sensing to monitor high spatiotemporal physiological stress from skin conductance level (SCL) and analyzed the association between the visual environment and the SCL in high-density environments. The multi-level visual environment was quantified from isovist and street view images. The most influential lags for each visual exposure factor were identified. Furthermore, multiple linear regression (MLR) and geographical random forest (GRF) were established to examine the effects of the lagged visual exposure factors on SCL. Particularly, the GRF can explore spatial nonstationary and complex relationships. The MLR ($R^2 = 0.466$) suggests that exposure to trees, sky, and sign symbols can relieve stress. The GRF with 5 visual exposure factors can explain 87.4% of the spatial variance of SCL. This study confirms the effectiveness of monitoring pedestrians' stress in high-density cities and the phased and non-instantaneous impacts of the visual environment. The results have practical implications in urban design at both district and site levels for a sustainable and psychologically friendly urban environment.

1. Introduction

1.1. Background

World Health Organization recently noted that the needs for improving mental health are high but responses are inadequate worldwide, and predicted that one in five people have suffered a mental disorder in the last decade (World Health Organization, 2022). The outbreak of COVID-19 is causing further negative psychological impacts on people (Grover et al., 2020; Saladino, Algeri & Auriemma, 2020; Serafini et al., 2020). Furthermore, rapid and intense urbanization exposes urban residents to more stress (Lederbogen et al., 2011; Weich, 2002). Therefore, it is essential to create a sustainable and healthy living environment to minimize the negative impacts on the mental health of urban residents. Promoting mental health and creating healthy cities have become the indicators and targets of the Sustainable Development Goals (SDGs) of the United Nations (SDG 3.4 and 11.3).

1.2. State of the art

Understanding the interaction between people and the environment is fundamental to urban planning strategies to promote healthy and sustainable living environments. Advances in wearable technology enable psychophysiological sensors to accurately and stably record individuals' physiological responses, thus further fostering the understanding of the effects of urban spaces on people's psychological experiences and people-oriented design strategies.

Based on wearable devices, the first idea of visualizing and mapping emotional data comes from an artist (Nold, 2009), and many scholars conducted a series of outdoor experiments to seek opportunities to reduce human stress levels in urban environments (Griego, Buff, Hayoz, Moise & Pournaras, 2017; Hijazi et al., 2016; Javadi et al., 2017; X. Li

* Corresponding author.
E-mail address: XIANG.Luyao@link.cuhk.edu.hk (L. Xiang).

[1] Both authors contributed equally to this work and should be considered co-first authors.

https://doi.org/10.1016/j.scs.2023.104695
Received 12 January 2023; Received in revised form 30 March 2023; Accepted 28 May 2023
Available online 2 June 2023
2210-6707/

et al., 2016; Mavros, Austwick & Smith, 2016; Neale et al., 2020) (W. Lin et al., 2020; Mangone, Capaldi, van Allen & Luscuere, 2017; Rogerson, Gladwell, Gallagher & Barton, 2016; Xiang, Cai, Ren & Ng, 2021). These studies proved the effectiveness and stability of wearable devices application in outdoor spaces and laid the theoretical and empirical foundation for further studies.

In addition, vision is the major source of the external information that people typically acquire, which largely affects human perception (Brakus, Schmitt & Zarantonello, 2009) and subsequent experience (Kalat, 2015). A series of experiments conducted outdoors have verified the impact of various visual characteristics on psychological perceptions, such as isovist (De Silva, Warusavitharana & Ratnayake, 2017; Hijazi et al., 2016; X. Li et al., 2016; Marianne & Knöll, 2017; Winz et al., 2022), architectural variation (Lindal & Hartig, 2013), the low or high-rise of the buildings (Mazumder, Spiers & Ellard, 2022) and the streetscape (X. Li et al., 2016; F.-C. Lin, She, Ngo, Dow & Hsu, 2021; Xiang et al., 2021; Zheng Chen, Sebastian Schulz, Xiaofan He & Yifan Chen, 2016). The visual environment is therefore an important diver of physiological stress. It is essential to understand its effects on physiological stress to facilitate urban planning strategies toward a psychologically friendly urban environment.

1.3. Literature review on physiological stress: insights from laboratory studies and drawbacks of current outdoor studies

A number of studies have analyzed the interaction between physiological stress and visual environment. In particular, physiological stress can be quantified by the general tonic skin conductance level (SCL). SC has been considered to constitute an objective assessment of sympathetic activity through the electric impulses on the surface of skin and sweat glands, which are affected only by the sympathetic nervous system (Jesper J. Alvarsson, Stefan Wiens & Mats E. Nilsson, 2010). SC contains phasic skin conductance response (SCR) and skin conductance level (SCL); the former refers to the faster changing of the signal, and the latter relates to the slower-acting ones. SCL can be computed as an average across longer intervals that typically range from tens of seconds to tens of minutes, depending on the environment and time. The higher the SCL, the greater the stress.

Therefore, SCL has been frequently used as a measure of physiological stress to understand the effects of the visual environment. The empirical studies focused on SCL are mainly from interior spaces and laboratories. Roger S. Ulrich et al. (1991) continuously monitored a series of physiological measures, including 10-minute changes in SCL response, and found that individuals who viewed natural settings experienced more rapid and complete recovery compared to the built settings. Stress recovery from nature views happened remarkably fast—in about 4 min. Huang, Yang, Jane, Li and Bauer (2020) found that stress levels showed different tendencies in the 7th minute after viewing concrete, grass, and tree landscapes. Yin, Zhu, MacNaughton, Allen and Spengler (2018) identified the different physiological stress performances from the same stress stimulus by evaluating time cost. Laboratory research verified that the changes in SCL are not instant responses to visual scenes and also noise (J. J. Alvarsson, S. Wiens & M. E. Nilsson, 2010). Its fluctuation depends on different types of landscapes and is a long-term effect of the stimulus.

Since these studies were conducted in controlled laboratories, the results can be different from those in the real built environment and have limitations to guide the real urban planning practice. Nevertheless, the characteristic of SCL from experiments in laboratories can still inspire the hypothesis that the earlier events (what subjects have seen in this study) can influence the current SCL within different scales and periods. For example, pedestrians will gain good physiological stress conditions after touring an urban park, and the effect will maintain for a while. After leaving the site and entering the street environment of hundreds of meters, this effect will be weakened. Therefore, taking the influential spatial lag of the physical elements into consideration is essential for establishing a deep understanding of how the built environment visually influences physiological stress.

In terms of the outdoor measurement of SCL, the majority of studies stayed at comparing of the differences between before and after experiencing various types of urban or greening spaces or various types of human behaviors (Kim, Yadav, Chaspari & Ahn, 2020; Mavros, J Wälti, Nazemi, Ong & Hölscher, 2022; Mir et al., 2023). According to the definition of SCL and the findings from interior experiments, it is essential to fully explore the spatiotemporal variations of SCL within urban environments. Furthermore, those outdoor experiments rarely consider the long-term effect of the visual environment. Besides, SCL responses to specific visual elements in urban areas, such as roads, buildings, and sky, have not been analyzed or quantified. Those limitations of the current outdoor studies bring challenges to the accurate understanding of the effect of the visual environment and effective spatial planning strategies to improve the mental health of pedestrians.

1.4. Analytical methods for exploring the relationship between visual environment and physiological data

As for the methods to associate the visual environment with physiological data, laboratory studies commonly adopted pathway or correlation analysis. For outdoor conditions, the environment is more complicated with unknown, diverse, and unstable changes. More advanced methods are thereby required to reveal the environmental impacts timely and spatially. In the outdoor environment, previous studies generally adopted global statistical models such as multiple linear regression (MLR) (Millar et al., 2021; Xiang et al., 2021) and machine learning (X. Li et al., 2016). Compared with the linear model, machine learning methods can consider nonlinear and complex relationships. However, those models regard the relation as instantaneous and spatially stationary for each point. Physiological stress can not only be affected by the environment at the specific locations but also the previous experience that happened in the surroundings. The effects of the visual environment can be continuous and spatially variant, while few studies have attempted to account for spatial heterogeneity when modeling stress as a function of geographical data. Hence, considering the spatially non-stationary impacts of the visual environment in the statistical model is significant for a more accurate understanding of the effect of the environment. Spatial machine learning that can consider the spatial non-stationary, nonlinear, and complex relationship, is therefore suitable for analyzing the impacts of visual environment on physiological stress.

1.5. Objectives

In order to address the above research gaps, this study aims to understand the impact of multi-level visual environments on physiological stress in outdoor environments using ambulatory technology and spatial machine learning. The application and utility of the findings of this study are anticipated to contribute to spatial optimization schemes and planning strategies to achieve healthier and more sustainable cities and communities.

The objectives of this study are as below:

1 To monitor the spatiotemporal variations of SCL in an outdoor urban environment.
2 To quantity the visual environment using both street view images and isovist.
3 To conduct a sensitivity test to identify the most influential lag distance for each visual impact factor.
4 To gain a quantitative understanding of the effects of various visual exposure factors on SCL using linear regression and spatial machine learning.
5 To provide urban planning recommendations to promote the mental health of pedestrians.

2. Materials and methods

2.1. Study area

Situated on the southeast coast of China, Hong Kong has the third highest population density globally (The World Bank, 2018). The confined living conditions caused by the high-density development are detrimental to the mental health of local residents. Hong Kong Mental Morbidity Survey shows that one in six of the local residents has a mental disorder, like anxiety or depression. This number increased to one in two in 2016 (The Mental Health Association of Hong Kong, 2016). Approximately 60% of the citizens claimed to have mental health issues in 2020 (MHA 2020).

Tsim sha tsui (TST) and Hung hom (HH), two districts on the Hong Kong Kowloon Peninsula with the highest building volume density, are chosen for the field trip. TSTS is a bustling commercial district, whereas HH is a residential community. TST is well known for its commercial vibe and draws a sizable number of tourists every day. TST is one of the busiest areas in Hong Kong and has few trees because of the vibrant business climate there. The majority of the initial section of the HH route is made up of undeveloped area, with only a few structures. Because there are few commercial activities along this route, it is calm and sparsely populated. The second part of the HH route is typical of the urban environment, featuring food markets, communal facilities, and high-rise residential buildings. The big stars in Fig. 1 indicate the gathering points for the pre-walk test. The lengths of the routes are 1.1 km and 1.3 km for TST and HH, respectively. At the black point, the data begin to be recoyrded. The location of the mid-walk test is also indicated by a small star on the map.

2.2. Visual exposure data

2.2.1. Isovist

Isovist has a long history in architecture and geography, as well as mathematics (Turner, Doxa, O'Sullivan & Penn, 2001). The definition of isovist is 'the set of all points visible from a given vantage point in space (Larry S. Davis & L.Benedikt, 1979). Isovist has been theoretically and empirically proved that it has a strong relationship with human behavior and psychological interaction with the environment (Appleton, 1975; Dawes & Ostwald, 2014a, 2014b; Dosen & Ostwald, 2016; Fisher-Gewirtzman, Burt & Tzamir, 2003; Fisher-Gewirtzman & Wagner, 2003; Yu, Gu & Ostwald, 2016).

We calculated 2D isovist and 3D isovist in Rhino 6, Grasshopper Decoding Spaces Toolbox developed by the team of Computer Science in Architecture at Bauhaus University (https://toolbox.decodingspaces.net/). The building models used for calculation were adopted from a previous study (Ren, Cai, Li, Shi & See, 2020). The maximum visual length is determined as 500 m, the visual height was 1.6 m, The basic settings of isovist calculation are summarized in Table 1.

The 2D isovists describe the characteristics of the visual area on a 2D floor plan, the parameters include isovist area, perimeter, compactness, circularity, occlusivity, the length of the visual radial line, the angle between the direction facing occupant and the mass center of an isovist polygon, etc. The 3D-volumetric isovists describe the proportion of each factor, including sky, object, ground, and visual volume (total length of all visual lines).

2.2.2. Street view factors

Apart from isovist, the street view factor (VF) is another important way to quantify the physical streetscape. Isovist reveals the geometric characteristics of the visual areas, but the accuracy of the calculation relies on the precision of the building model. Furthermore, models of other urban elements, such as greenery, are hard to obtain and built. Street view images can compensate for the drawbacks of isovist, providing additional information about the visual content. Therefore, this study combined the isovist and street view factors together to build

Table 1
The basic settings of isovist calculation in Decoding.

Visual height	1.6 m
Viewing range	500m
Horizontal Viewing angle	60 °
Vertical viewing angle	55 °
Vertical angle offset	−2.5 °

Fig. 1. Study area and experimental routes: (a) TST route, (b) HH route.

a multi-level visual environment.

VF was determined as the percentage of the class pixels and the total pixels of the street view image. We adopted a pre-trained network based on the Cambridge-driving Labeled Video Database (CamVid) (Brostow, Fauqueur & Cipolla, 2009) and the Deeplab v3+ network (Chen, Zhu, Papandreou, Schroff & Adam, 2018) with weights initialized from a pre-trained Resnet-18 network. The view factor of the seven most common and basic elements in urban areas, namely, sky, building, road, sign symbol, car, people, and tree were extracted from the images.

We divided experimental routes with 4 m intervals, and there were 548 sample points in total. 28 visual exposure factors were finally retrieved for each point, of which 21 were from isovist and seven were from street view images. The detailed definition and spatial distribution of the visual exposure factors can be found in Table S1 and Figure S1 in the supplementary information (SI).

2.3. Experimental details

2.3.1. Subject enrollment and experiment time

An online announcement with a 60 HKD reward for each person was used to recruit participants. The range of ages was set at 18 to 35. There were 103 participants in total ($M = 51$, $F = 52$). The participants' average age is 26 (SD = 5). Experimental routes were assigned to the participants at random. Lastly, 51 people took the TST route and 48 people took the HH route, respectively. Four individuals ended the experiment midway due to personal reasons.

Taking into account the extreme weather in Hong Kong, the experiment was carried out from December 2018 to May 2019, when the weather was relatively pleasant (minimum air temperature = 17.67 °C, standard deviation = 3.99 °C, maximum air temperature = 24.08 °C, standard deviation = 4.28 °C; data source: HKO, available at https://www.hko.gov.hk/en/index.html). Two time periods, 10:00 to 12:00 am and 2:00 to 4:00 pm, were chosen for experiments on weekdays.

2.3.2. Experiment design

Three people participated simultaneously in the experiment on each environmental day. Each participant made their own way to the gathering spots. After receiving an overview of the experiment upon arrival, the participants were asked to sign a written consent form for their voluntary participation.

The experiment began with 100 s of standing posture relaxation retreatment (Chatterjee et al., 2018), this value is used as the SC baseline for subsequent data processing. In the first ten minutes, the participants viewed the corresponding landscapes from a seated position. After that, an experimental instructor led the participants on a walk that lasted for forty minutes.

The SC was recorded continuously at a frequency of 10 HZ throughout the experiment. Additionally, self-reports of perceived valence and arousal conditions were collected three times throughout the experiment—at the beginning, middle, and end. The experiment takes about 90 min to complete. Fig. 2 provides an overview of the experimental procedure.

2.4. Mobile data collection

A dedicated GPS device (Garmin GPSmap 62 s) was attached to the shoulder of the participant at a frequency of 1 Hz. It collected the geographic coordinates of the participant and the corresponding time-stamps as they walked the predetermined route. The real-time SC data, street views, and isovist data were then combined with the locational data.

This study used clinical devices for the acquisition of the psychological stress data owing to the high accuracy of the raw data and the professional post-processing system. The Shimmer 3 GSR+ device (Shimmer, www.shimmersensing.com/) is used to measure skin conductance. It has been clinically tested and demonstrated high validity and accuracy (Gatti, Calzolari, Maggioni & Obrist, 2018).

2.5. Physiological data processing

Ledalab 4.8.3 toolbox (www.ledalab.de) was used to analyze each recording. Based on the default parametric parameter, we used continuous deconvolution analysis (CDA) to separate the SCL and SCR from the raw data. The Event-Related-Activation tool in Ledalab calculates and exports the average SCL for each sample every four seconds.

We standardized SCL after separating the raw SC data to exclude individual differences. The baseline and the range for each individual are relative, that is, 15muS can be an extremely high SCL for one individual, but only the baseline SCL for another. There is no universally agreed method. The study adopted the range-corrected scores introduced by Dawson, Anne M. SCHELL and FILION (2001), computing the minimum SCL during the baseline (or rest period) and the maximum SCL during the most arousing period. The SCL of the participants at any other time, in this study, can be delineated as a proportion/percentage of their maximum range of individual psychophysiological response using (Eq. (1)):

$$\mathrm{SCLj}^{'} = \frac{SCL_j - SCL_{baseline}}{SCL_{Max} - SCL_{baselinemin}} \tag{1}$$

where $SCl_j{}'$ is the standardized SCL score at the aggregation point j. SCL_j is the extracted value at point j, $SCL_{baselinemin}$ refers to one's minimum SCL during baseline recording, SCL_{max} refers to one's maximum SCL level during the whole experiment.

2.6. Statistical analysis

We aggregated the data by combining the visual exposure factors and physiological data of 99 participants, with an interval of 4 m for further statistical analysis. All participants' SCL values were averaged for the same geo-coordinate point, which would be regarded as the response variables. Meanwhile, the 28 visual exposure factors from both street view images and isovist at the corresponding geo-coordinate would be used as potential predictor variables.

2.6.1. Identifying the most influential lag distance

SCL relates to the slower-acting components, showing phased changing over long intervals according to different environments

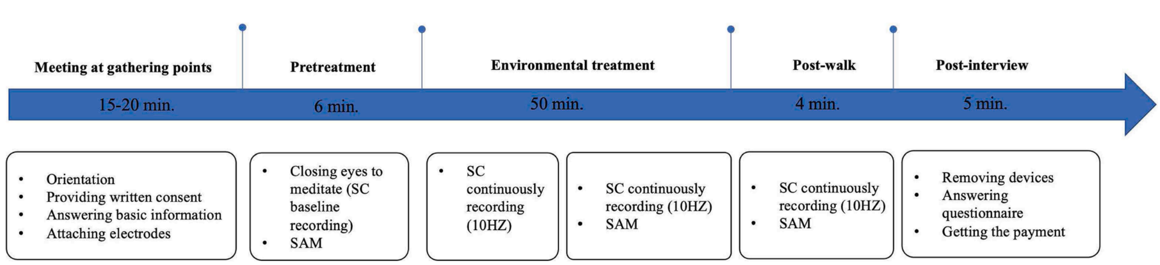

Fig. 2. overview of the experimental procedure in the real urban environment.

stimuli, typically ranging from tens of seconds to tens of minutes, which can be further reflected in distances from dozens to hundreds of meters. Therefore, it is essential to evaluate the most influential time interval or distance of each visual exposure factor to exclude the impact of long-term environmental signals on stress and acquire visual sensitivity. To detect the most influential distance and verify the hypothesis of time lag, we conducted a sensitivity test of different lag distances inspired by the 'space for time' concept (Y. Li et al., 2023; Shi, Ren, Lau & Ng, 2019) (Fig. 3). The maximum scale of the lag distance was set as 500 m and the interval as 20 m, which corresponded to the scale of the general community and buildings in Hong Kong, respectively. There were 26 lag distances in total including zero (no lag). The mean value of all the visual exposure factors within each lag distance was calculated. The same factor calculated within different lag distances was regarded as different variables. For example, tree view factors calculated using 20 m and 40 m lags were regarded as two different factors in this study. The 28 visual exposure factors needed to be calculated using the 26 different lags.

Correlation analysis was conducted to gain the correlation coefficient (r) between the mean visual exposure factor within the 26 lags and the SCL' at the pedestrian point to detect the most influential lag distance. For point j, the largest R^2 for each lagged visual exposure factor can be expressed as (Eq. (2):

$$\mathrm{Rmax}^2 = Max\left\{\left[r\left(\frac{\sum_{i=1}^{n} VE_{ij}}{n},\ \ SCL_j\right)\right]^2\right\} \tag{2}$$

where r refers to the correlation coefficient, n means the number of intervals that range from 0 to 25, VE_{ij} represents the i_{th} visual exposure factor contained in the lag distance since point j, SCL_j is the average of all participants' physiological stress at point j. When the Rmax^2 of each visual exposure factor was identified, the corresponding lag was regarded as the most influential lag distance for the factor.

It can be assumed that the Rmax^2 can be low for some visual exposure factors. To only include influential visual exposure factors in further modeling, this study set 0.1 as the threshold, and factors with Rmax^2 lower than this value were excluded. A spatial moving window approach was then performed on each remaining factor and the most influential lag distances were regarded as the window size (Fig. 4). For each visual exposure factor, only the mean value within the lag distance corresponding to the Rmax^2 was selected as the potential predictive variable and included in the next stage of the statistical analysis (Shi et al., 2019).

2.6.2. Multiple linear regression

The multiple linear regression equation is shown as (Eq. (3):

$$SCL^{'}j = \alpha_1 VE_1 + \alpha_2 VE_2 + \ldots + \alpha_n VE_n \ + \gamma + \varepsilon \tag{3}$$

where SCL'_j is the averaged physiological stress across all participants at the aggregation point j. VE denotes the lagged visual exposure factors. α1…, αn are the coefficient estimates of the metrics VE1, VEn at point j. γ is the model intercept, and ε is the residual. The MLR model was constructed based on the visual exposure factors with the most influential lag distance retrieved from section 3.5.1. We used stepwise linear regression. The least correlated variable is eliminated from each iteration of multiple regression, and all significant variables are included in the resultant model. In order to include significant and non-collinear factors, we refined the independent variables by adopting the following rules: p-value < 0.05 and VIF < 5.

2.6.3. Geographical random forest

Random forest (RF) is a classical and popular machine-learning algorithm that consists of multiple decision trees (Breiman, 2001). Compared with other machine learning techniques such as K-Nearest Neighbors, Naive Bayes, and Support Vector Machines, RF has the ability to handle mixed data types and missing data, non-linear decision boundaries, and provide feature importance ranking. Besides, since the RF makes predictions based on multiple decision trees, it generally shows high accuracy levels (Chung, Xie & Ren, 2021) and rarely has the overfitting issue. Therefore, the RF is a suitable machine learning approach for modeling and interpreting SCL based on the multi-dimensional visual exposure dataset in this study.

The original RF regression is a global model that conducts regression for the entire data domain. Recently, a geographical RF (GRF) model has been developed as an extension of the RF to incorporate spatial non-stationarity, which is similar to Geographically Weighted Regression (GWR) (Fotheringham, Brunsdon & Charlton, 2003) that decomposes the global OLS model to local computation. Therefore, GRF is a bridge between machine learning and geographical models, taking advantage of the predictive power of the RF and the spatial non-stationarity of the GWR. We adopted the GRF in this study to consider the effect of surrounding visual environments as well as the non-linear relationship.

The GRF was developed based on the decomposition of the RF to several local sub-models (Eq. (4)). This means that for each position i, a local RF is calculated, including n nearby observations. Therefore, each

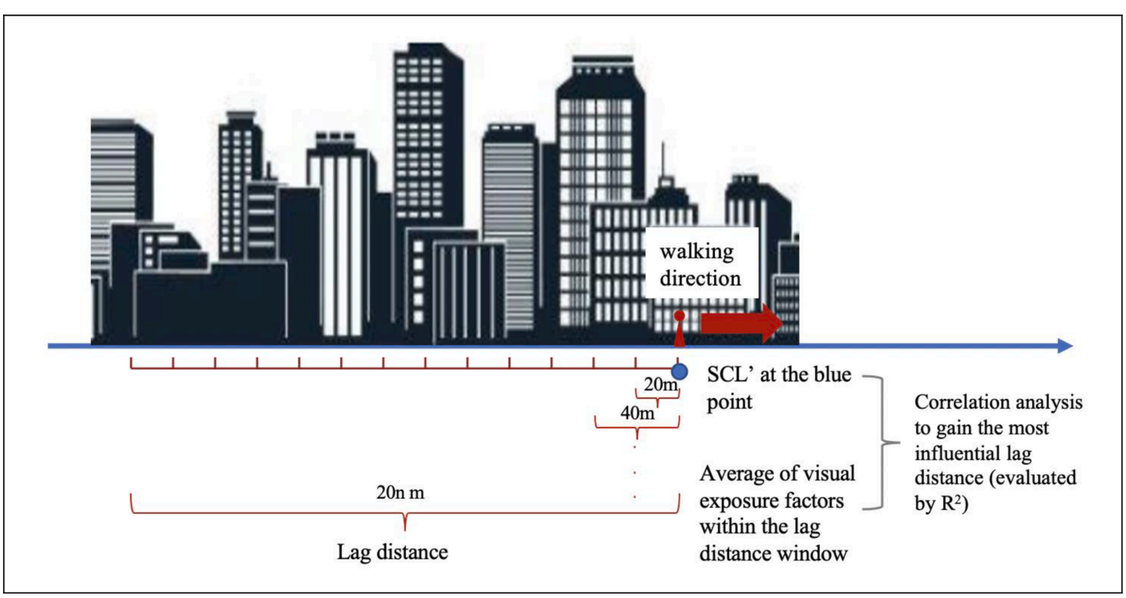

Fig. 3. Workflow of identifying the most influential lag distance. The red arrow represents the walking direction of participants.

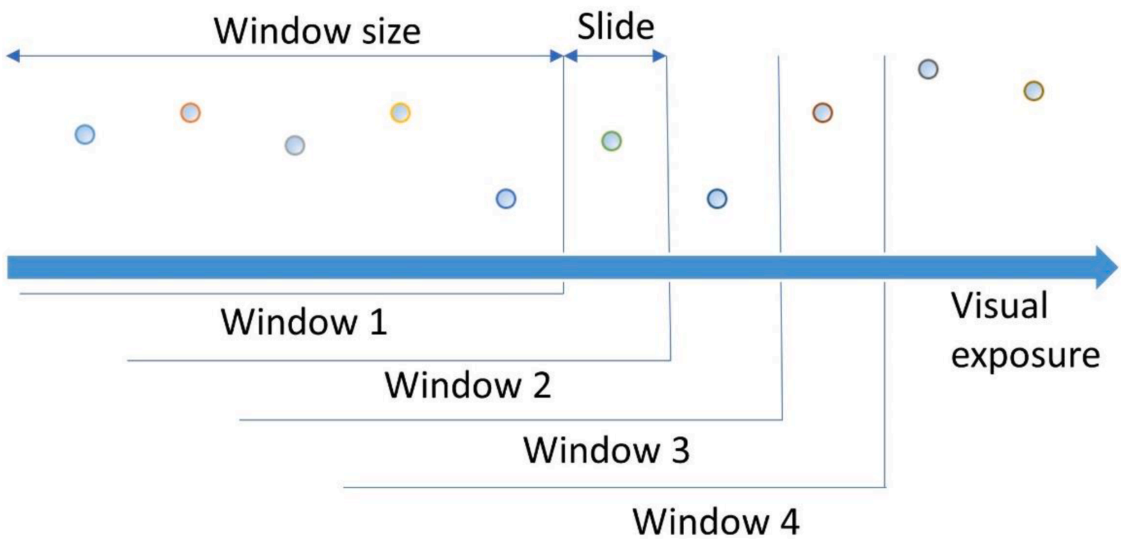

Fig. 4. Spatial moving window approach to acquire the lagged visual exposure.

local RF model has its own performance, predictive power, and variable importance at each training data point. Accordingly, the model is evaluated locally for each observation.

$$Y_i = a(u_i, v_i)x_i + e, i = 1 : n \tag{4}$$

where $a(u_i, v_i)x$ is the prediction of an RF model calibrated on location i, and (u_i, v_i) are the coordinates. A sub-model is built for each data location, considering only nearby observations.

First, the observations were randomly divided into training sets and validation sets in a ratio of 80% to 20%. The model was developed using the training data sets. The GRF was performed using the 'SpatialML' package in R (Georganos et al., 2018); "SpatialML." R Foundation for Statistical Computing. This model contains two sets of necessary parameters. The first set comes from the original RF, including the number of trees, the number of predictors to sample as candidates at each split, and the minimum leaf size. These parameters were tuned using a Bayesian optimization from the global RF model and the parameter values from the optimization were used to train the local models.

The second set is geographical parameters, including coordinates of the observations, and the area in which the sub-model covers (kernel) (Kalogirou, 2016). In this study, the kernel was defined by a circle with a distance of maximum distance (bandwidth) (Brunsdon, Fotheringham & Charlton, 1998; Fotheringham et al., 2003). In this study, we tuned the kernel from 20 m to 300 m with a 20 m interval and determined the optimal kernel value based on the R^2 and MSE of the local model.

Finally, the optimal GRF model can be established from the optimal parameters, and the validation data were fed into the retrieved trained model to acquire the predictive value. The retrieved predictive model was evaluated by R^2, RMSE, and MAE for both the trained data and validation data.

3. Results

3.1. Basic information about the participants

For the TST route, there were 51 participants, including 22 were males and 29 females. The average age is 25.80 (SD=4.75). For the HH route, 48 people participated, including 25 males and 23 females. The average age is 26.27 (SD= 5.35). The overall mean familiarity of two routes is 3.53 (SD=1.57), which is located within the Likert scale (ranging from extremely not familiar 1 to extremely familiar 7). The mean familiarity is 3.69 for TST (SD=1.62) and 3.35 for HH (SD=1.51). The participants were not very familiar with the study area. They were curious about the routes to some extent and did not quickly lose interest during the walk.

Participants did not feel much stress due to wearing Shimmer devices when walking (Mean=2.04, SD=1.06), and the feeling of discomfort from just looking ahead was slightly greater (Mean=2.64, SD=1.36). This indicates that the rules of the experiment did not significantly influence the participants.

3.2. The SCL scale statistics

The results of the paired t-test showed, as expected, that walking in an urban environment significantly affected the SCL of the participants ($M_{pre\text{-}walk} = 3.44$, $M_{mid\text{-}walk} = 5.706$, $M_{post\text{-}walk} = 6.375$, $p<.001$). The arousal increased after walking in the experimental routes. It can be noted that the increasing trends are the same for the two routes between pre-walk and mid-walk, but different between mid-walk and post-walk. The SCL of the participants in the TST group decreased after the second part, while for the HH group, the SCL increased gradually (Table S2 in SI).

As expected, the SCL baselines for the two routes showed no significant differences (MTST =4.267, SD=3.464, MHH = 4.708, SD=4.223, F(1,97)=0.325, $p>.1$). After the standardization of the SCL, the data can be compared between different groups. The results of the ANOVA t-test revealed that the participants had significantly higher SCL' on the TST route compared to the HH route (F(1,97)=10.869, $p<.01$). The mid-points separated the routes into two parts. There is evidence that the major difference between the two routes came from the first part (MTST =0.74, SD=0.15, MHH = 0.45, SD=0.27, F(1,97)=39.75, $p<.01$). The second part of each route has similar effects on SCL', in which the mean value did not show significant differences (MTST =0.68, SD=0.14, MHH = 0.62, SD=0.35, F(1,97)=1.624, $p>.1$) (Table S2 in SI).

Fig. 5 indicates the spatial distribution of the SCL for both routes. The participants showed significantly higher SCL' at the end of the experiment, compared to the beginning of the walk. This indicates that walking around the city can increase the arousal of pedestrians. However, the spatiotemporal variations of SCL' for the two routes are different, which can be explained by different urban elements and morphological characteristics of the streets.

3.3. Influential lag distance

Although the relationship between each predictor and SCL' maintains the same direction for all lag distances throughout the process, R^2

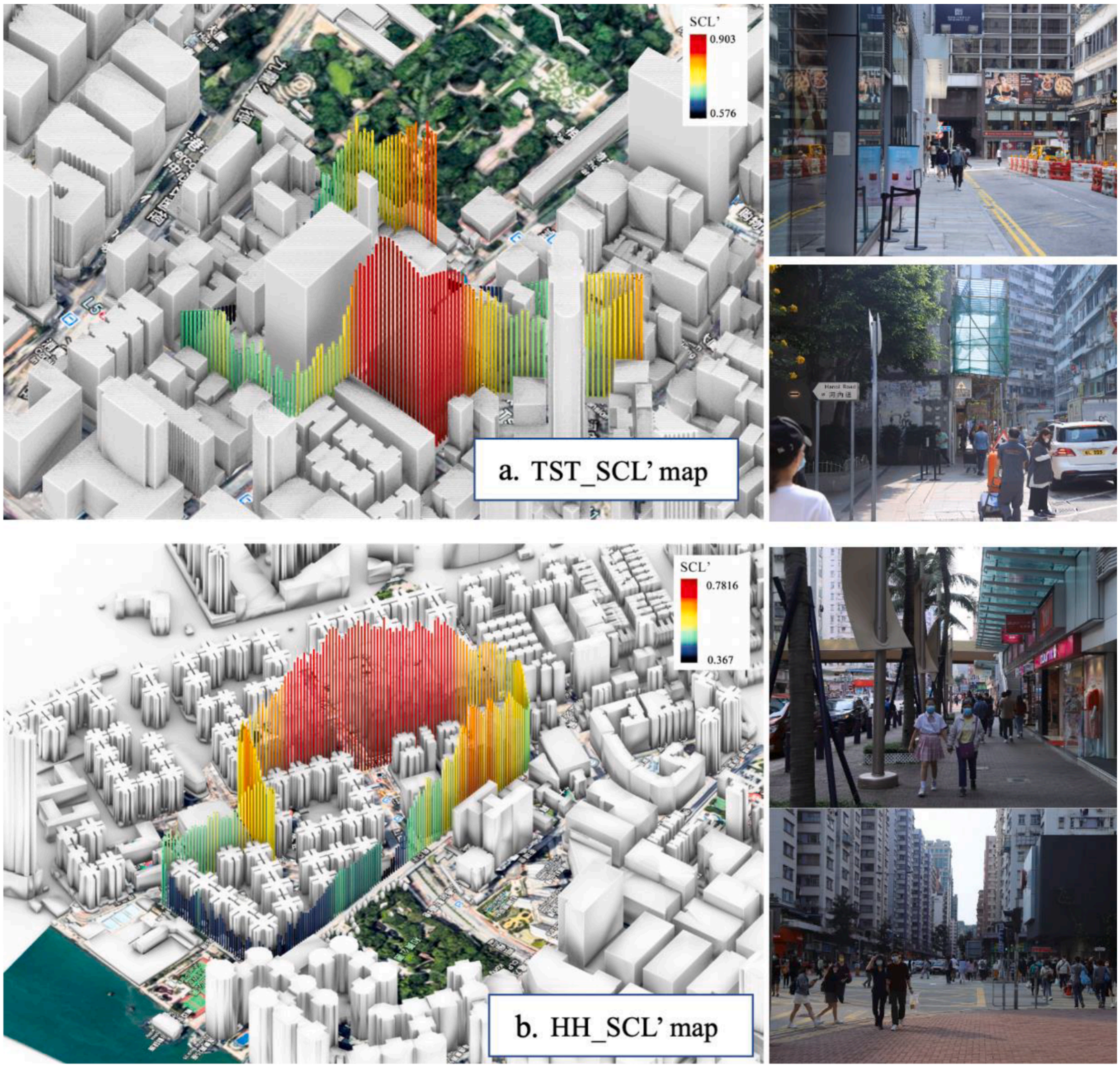

Fig. 5. Spatial distribution of SCL for (a) TST and (b) HH.

shows evident fluctuations. Taking the Road view factor (RVF) from the street view images as an example, R^2 increases along with the expansion of the distance, however, after the 160-meter threshold, it decreases rapidly (Fig. 6). When the average for predictors was calculated for a longer distance, R^2 gradually increases and reached the maximum.

Correlation analysis shows that the values of the R^2 of all visual exposure factors from 2D isovist are low, therefore, they are excluded in the further MLR and GRF analysis. The 2D isovist is mainly about the very detailed information of geometric characteristics of the visible area. The complicated information passes from sensory memory to short-term memory and long-term memory, and the number of perceptual details stored decreases (Brady, Konkle, Alvarez & Oliva, 2008), which was reflected by the relatively lower R^2 of 2D isovist.

For the rest visual exposure factors from 3D isovist and street view, nine visual exposure factors remain with R^2 larger than 0.1. The most influential lag distance and the corresponding R^2 of the remaining factors (Table 2). Among all the factors, the sky view factor of 50 m lag has the largest R^2 of 0.55, whereas the object proportion from 3D isovist has the lowest one.

3.4. Resultant models

3.4.1. Multiple linear regression

A total of 136 points for the HH route and 143 points for the TST route were reported finally. Table 3 shows the results of the MLR model. After the stepwise regression, five lagged visual exposure factors are significant and are non-collinear (VIF<5). The residual conforms to the normal distribution; therefore, the final model is effective and stable. The model already explains almost 46.6% variation in the measured SCL'. The results indicate the significance of street view and isovist in explaining the spatial variation of SCL'.

The increasing order of the effectiveness of the remaining visual exposure factors of the MLR model is: TVF, RVF, SSVF, sky proportion, and object proportion. Among the five predictors, three of them influence SCL' in a negative way, which are Sky3D, SSVF, TVF. TVF has the largest St. coefficients (−0.260) while Sky3D has the lowest (−0.181) one. The remaining two predictors, Obj3D and road view factor (RVF) are all positively related to SCL'.

3.4.2. Geographical random forest

Based on the selected five predictors, the optimal set of parameters was determined through the tuning process. The number of trees is 80, the minimum leaf size is one, and the number of predictors to sample is one. In the optimal global model, the R^2 is 0.840, RMSE is 0.024, and MAE is 0.017. the values of the parameters were further used to train the local models of the GRF.

In the GRF model, the bandwidth was tuned, and the 160 m bandwidth is associated with the highest R^2 and smallest MSE (Fig. 7). We

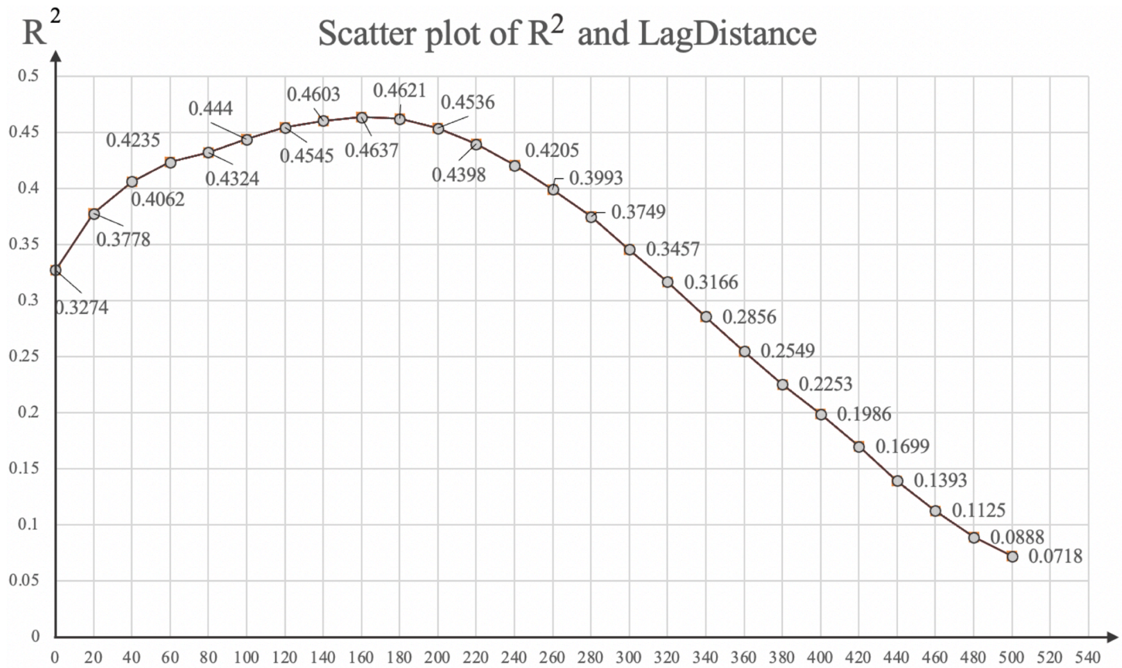

Fig. 6. Example of R^2 variation of RVF.

Table 2
Influential lag distance and corresponding R^2 for each predictor/.

Predictor	Influential lag distance (m)	R^2
3D isovist		
Sky proportion (Sky3D)	300	0.381
Object proportion (Obj3D)	400	0.131
Ground proportion	220	0.265
Visual volume	280	0.442
Street view		
Sky view factor (SkyVF)	200	0.550
Building view factor (BVF)	40	0.486
Road view factor (RVF)	160	0.464
Sign symbol view factor (SSVF)	100	0.254
Tree view factor (TVF)	80	0.477

Table 3
The resultant MLR model for interpreting the visual effects on SCL'.

predictor variables	standardized coefficients Beta	Sig.	VIF
intercept		.000	
Sky3D_300m	−0.181	.002	2.259
Obj3D_400m	.176	.004	2.365
RVF_160 m	.242	.000	2.598
SSVF_100 m	−0.232	.000	2.009
TVF_80 m	−0.260	.001	4.227

thereby determined the 160 m distance as the optimal kernel value. Based on the five predictors and optimal hyperparameters, the geographical RF model can be therefore established. The global mean R^2 of the trained geographical RF is 0.874 and MSE is 0.001, which shows higher predictive ability than the MLR and the global RF model.

The established model was further applied to the validation dataset. By comparing the predicted and the actual SCL in the validation dataset, R^2, RMSE, and MSE were identified to be 0.869, 0.036, and 0.001 respectively, indicating a satisfying accuracy of the established model and the potential of predicting SCL for new subjects by only using five visual exposure factors (Sky3D_300 m, Obj3D_400 m, RVF_160 m, SSVF_100 m, TVF_80 m) (Fig. 8).

Local R^2 reflects the accuracy of the model. Fig. 9 shows the map of its distribution. For the HH route, the value varies from 53.73% to 95.79% (M = 85.29, SD=7.09), for the TST route, the value varies from 57.89% to 95.30% (M = 84.85%, SD=7.49).

It can be seen that the high and low values occur at different locations for TST and HH routes. For the HH route, high R^2 is located centrally at the beginning stage of Tak on St, and at the end of the whole route. These two locations are mainly commercial areas compared to other sections. For the TST route, high R^2 is located more concentrated in the middle of the route, with a moderate commercial atmosphere. The first part of this stage is with a narrow and quiet environment, while the second part is the main road. Local R^2 shows different patterns in residential and commercial areas. For the commercial areas, visual elements with commercial characteristics, such as sign symbols, play an important role in increasing the R^2. In terms of residential areas, the locations with more trees and sky proportion have larger R^2.

In terms of the importance of the predictors, for the HH route, it can be noticed that all predictors are relatively more important in the second stage of Tak On St than other streets. The highest values of incMSE of SSVF, SkyVF, Obj3D_400 m appear on it, which ranges from 21%−26%. Especially, for the Obj3D_isovist, the values of other streets are much lower than Tak On St. The highest value occurs after the biggest crossroads along the route. For RVF and TVF, the highest incMSE value appears on the starting stage of dyer ave, where the participants turn right and enter an uphill road. It can be noticed that the importance of TVF is higher at this location from Fig. 10. Compared with the HH route, the distribution of high incMSE value of the TST route is more scattered for each predictor. The beginning of the route has a relatively lower value for all predictors. For the RVF, the highest value exists at the corner of Mody Rd and Nathan Rd, where the environment changes a lot, from the narrow street to the wide main city road surroundings. Similar to RVF, the highest incMSE of TVF also occurs at the corner of two roads. For other predictors, the high value is located on Hankow Rd.

With the variation of the incMSE values, it could be noticed that the two routes keep a similar level that the average. The mean value of TST is 2.949, while the mean value of HH 2 is 3.182. Among all the variables, RVF and SVF have a relatively larger variation of incMSE than other variables. The large variation of incMSE of RVF is caused by the

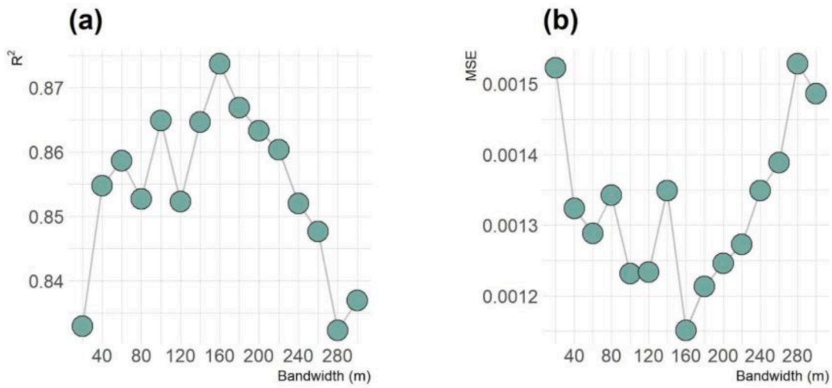

Fig. 7. the R^2 and MSE at different bandwidths scale.

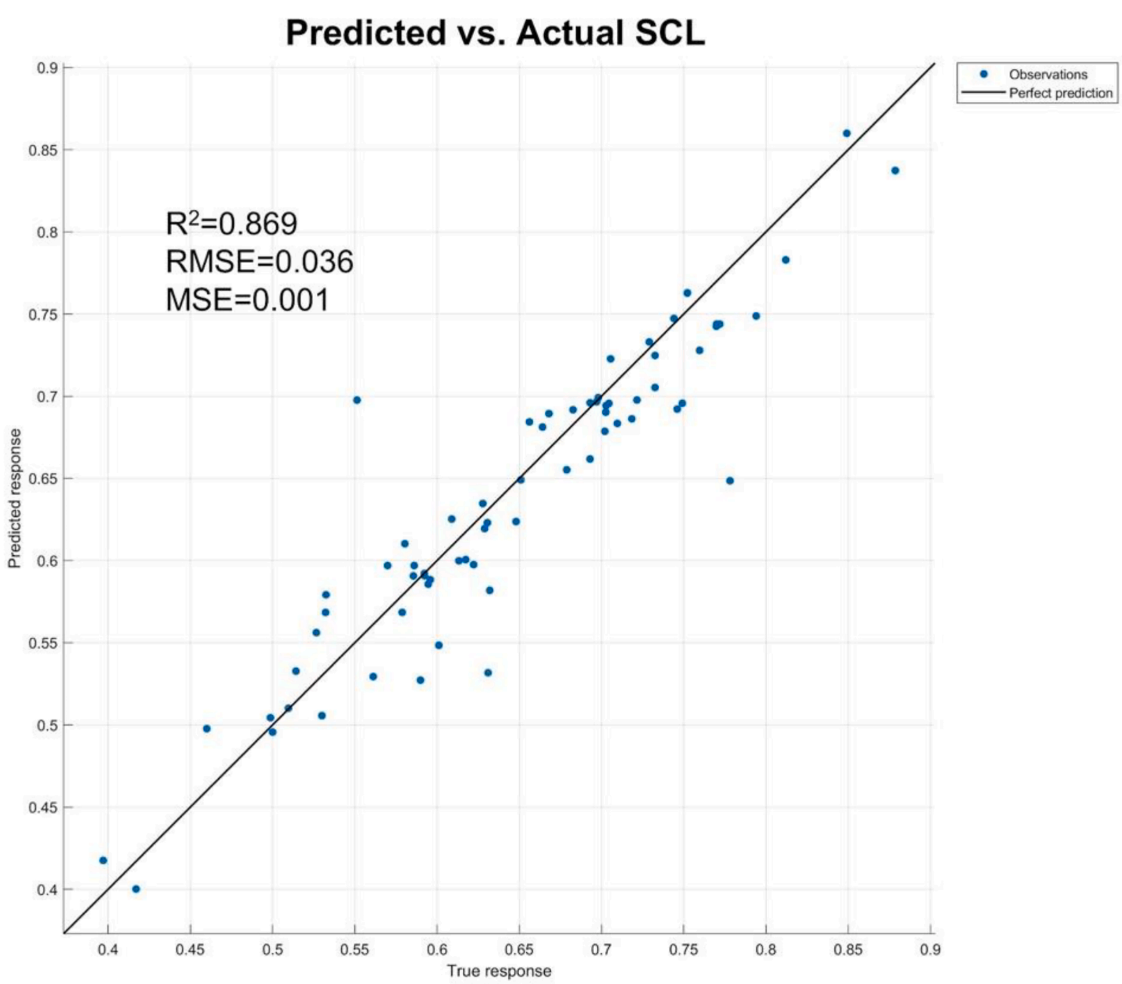

Fig. 8. predicted and true physiological stress response from the final predictive model.

complicated and various conditions of road within the experimental routes, which contain different human activities and traffic conditions.

Table 4 shows the statistical results of incMSE's of each predictor. Sky3D has the largest incMSE, while SSVF has the smallest for both routes. It indicates that Sky3D_300 m is the most important predictor that influences SCL' in this model, and SSVF_100 m is the least important one. Followed by Sky3D_300 m, TVF_80 m is the second most important one with the incMSE of 17.846 and 17.425 for the two routes respectively.

4. Discussion

4.1. Model interpretation

The MLR interprets 46.6% of the variation of the SCL. 2D isovist factors are not influential and are excluded from the resultant model. Only predictors from 3D isovist and street view factors remain in the final model, and it can be noticed that the predictors from 3D isovist and street view factors share some overlapping information, therefore, the 3D isovist ground factor is replaced by RVF. Among all predictors, TVF is

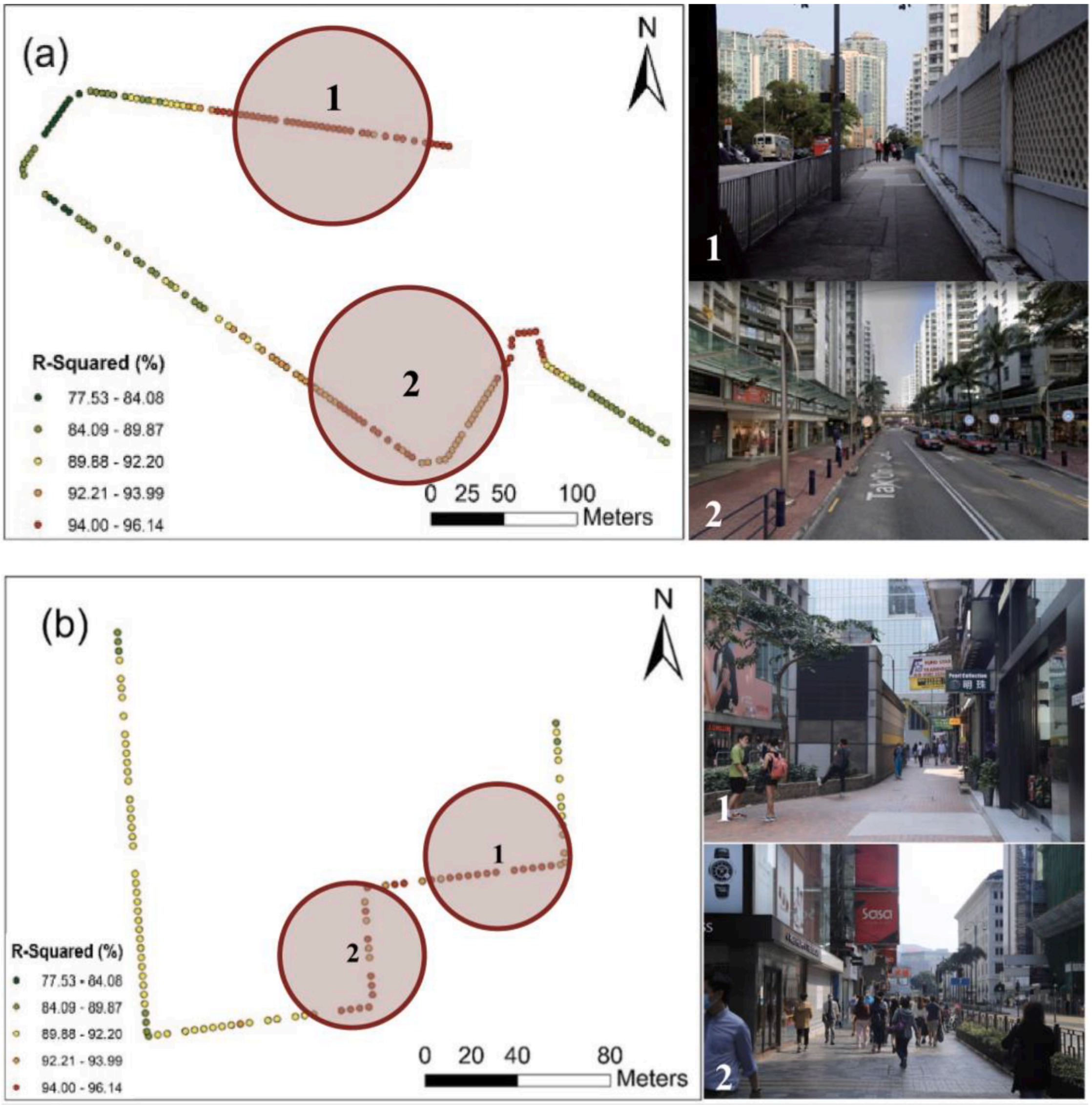

Fig. 9. Local R-squared value of HH (a) and TST (b) route.

the most important one that influences physiological stress. More trees within the visual area can be helpful to relieve physiological stress. Together with TVF, Sky3D, and SSVF also negatively affect stress. Pedestrians feel less stressed when their visual fields are more open to the sky or natural landscapes, which is in line with the previous studies in a high-density city such as Hong Kong (Xiang et al., 2021). The open sky in the crowded street is a kind of natural source that can provide 'soft fascination', which draws people's attention relatively effortlessly and is compatible with people's needs. It is interesting to see that SSVF helps relieve physiological stress, this could be understood from the perspective of attention restorative theory (Kaplan & Kaplan, 1989; Stephen Kaplan, 1983), that the sign symbols on the street are fascinating and allows 'effortless attention'. They may have sufficient scope to maintain interaction so that pedestrians are not bored, or they may simply be more in tune with people's interests.

The GRF model has a R^2 of 0.874 and shows a strong ability in the prediction of physiological stress. The distribution map of local R^2 shows the model has good performance in some parts of the routes, which means the results of GRF have better reference meaning for urban design at these locations. In terms of the importance of each predictor, Sky3D is the most important predictor that influences SCL' and SSVF is the least important one in this regression case. By combining the R^2 distribution with incMSE distribution maps, we can propose evidence-based urban design recommendations for better psychological experience and less physiological stress at the street level.

4.2. Comparison with previous studies

Combined with previous studies worldwide, the effects of visual environment on long-term stress (SCL) and short-term emotion (SCR) are summarized in Table 5 (Hijazi et al., 2016; Knöll, Neuheuser, Cleff & Rudolph-Cleff, 2017; X. Li et al., 2016; Xiang et al., 2021). Visual exposure factors play different roles in promoting emotion and relive long-term physiological stress. It can be noticed that TVF, sky proportion, object proportion, and SSVF are the three common factors that influence both emotion and physiological stress. Sky proportion, object proportion, and TVF play the same role in promoting pedestrians' psychological experience, while SSVF affects SCL and SCR in different ways. RVF has no significant effect on emotion but is positively correlated with SCL. The higher the RVF, the more likely it is to trigger physiological stress. The common findings from existing studies confirmed the validity of the results of this study.

Apart from the common findings from previous studies, this study determines the most influential lags of different visual exposure factors

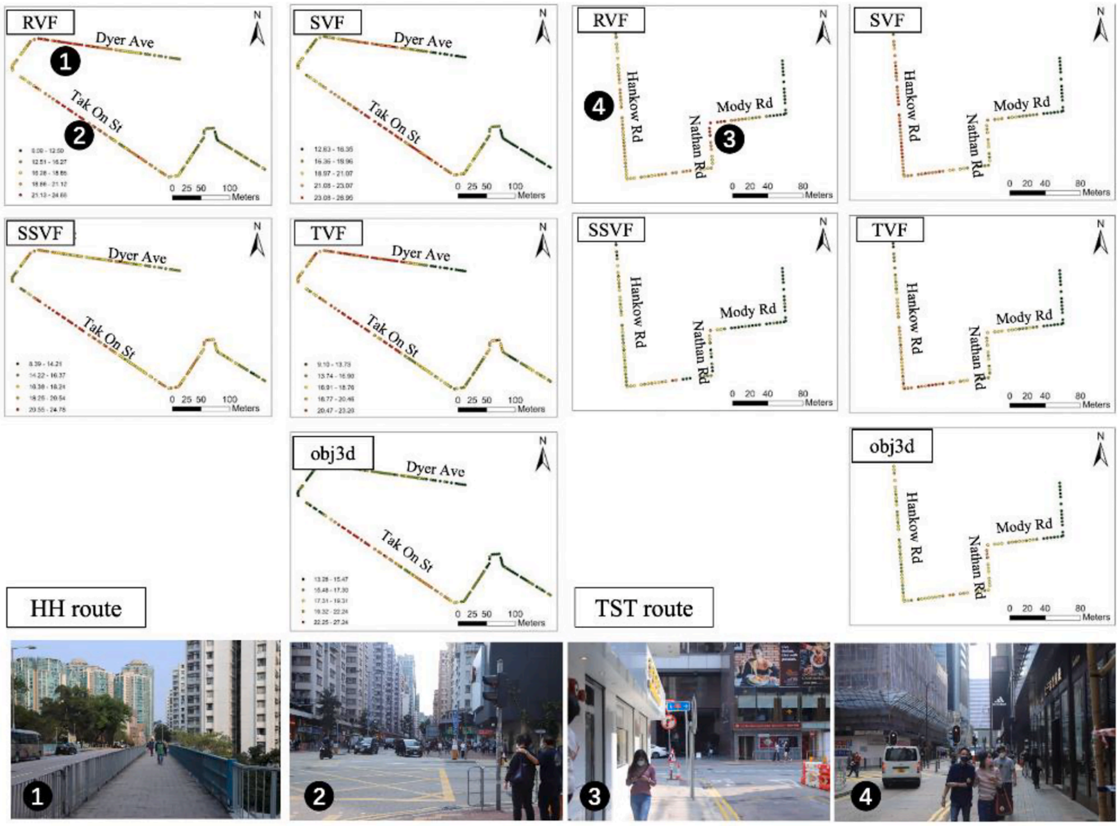

Fig. 10. incMSE distribution maps of the five selected variables for HH and TST routes.

Table 4
incMSE statistical results.

	HH		TST	
	M	SD	M	SD
Sky3D_300m	19.767	3.328	19.935	3.248
Obj3D_400m	17.299	2.553	17.263	2.615
RVF_160 m	18.005	3.311	17.719	3.550
SSVF_100 m	17.178	2.484	16.997	2.419
TVF_80 m	17.846	3.067	17.425	3.080

Table 5
Summary of the effects of visual exposure on SCL and SCR.

	Emotion (SCR)	Physiological stress (SCL)
Sky3D	Positive correlation	Negative correlation
Obj3D	Negative correlation	Positive correlation
Visual volume	Positive correlation	N.A.
Tree view factor	Positive correlation	Negative correlation
Sign symbol view factor	Negative correlation	Negative correlation
Road view factor	N.A.	Positive correlation

and identifies that pedestrians' SCL is more sensitive to TVF and SSVF. Besides, this study more adequately models the impact of the visual environment using spatial machine learning techniques and considers the spatial non-stationary, and indicates that the local models in commercial land use are stronger than those of residential land use.

4.3. Implications to urban design at district and site levels

The 6.2.34–6.2.48 sections in Chapter 11 of the Hong Kong Planning Standard and Guidelines (Department, 2015) fail to provide detailed and quantitative standards to promote mental health. This study can partly complement existing policies at both district and site levels.

At the district level, the influential lag distance provides the quantitative reference of design scales of each factor. The designers should pay more attention to the factors with smaller influential lags since pedestrians are more sensitive to them. In this study, TVF and SSVF have the most influential lag distance of fewer than 100 m, so priority should be given to their design and optimization. Additionally, the lag distance value can be a practical reference of the basic spatial unit for urban design. For example, as the positive effects from exposure to trees and sky have the most influential lag distances of 80 m and 300 m, beyond these distances, the positive effects would decrease. Therefore, it is suggested to adopt the spatial grid of 80 m and 300 m to achieve the most effective visibility of trees and sky, respectively, so as to maximize the relief effect from trees and sky (Fig. 11). Besides, urban designers can refer to the results from MLR and GRF models to identify the dominant visual factors and adopt corresponding design strategies to adjust the

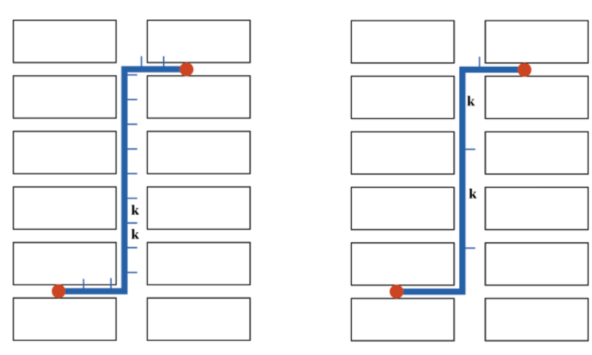

Fig. 11. Basic spatial grid to adjust TVF and SkyVF. The red points are random points on the street to ensure psychological comfort from one to another.

values of the factors. Moreover, the GRF model provides information about the spatial difference in importance ranking of visual exposure factors, which is helpful when solving the problem at any specific location. For instance, designing or optimizing RVF is more effective in the corner of Mody and Nathan Road in the HH route.

At the site level, to increase the sky proportion within visual areas for increase psychological comfort, it is critical to take design methods to optimize the building layout, podium, and façade, such as creating concave spaces on the building façade to increase visual volume, when appropriate, a terraced podium design can be adopted to decrease the obstacle from podium parts (Fig. 12).

4.4. Limitations and further study

Several limitations exist in this study. First, this study was conducted for a certain group of people in a controlled environment. The participants in the experiments were all young, healthy adults. Besides, as our experiment was conducted on a real urban street, we attempted to optimize the experimental condition to obtain more ideal results. To be specific, we selected a specific period under stable and similar weather conditions and limited the desire of the participants to a certain extent during the walk. Therefore, the results of this study may not be applicable to other people groups in different urban environments. Moreover, the statistical models were established based only on visual exposure factors. Other potential influences, such as sound, air pollution, and nighttime situation have not yet been taken into account.

There are several future research plans based on the current study. First, we plan to adopt more advanced ways to acquire other psychophysiological data, such as the EEG and EOG for a more comprehensive understanding of how stress changes over space and time. Furthermore, in order to make up for the incomplete variables in the current statistical model, control variables including sound, air pollution, time, weather, etc., will be considered in future work. We also plan to adopt video clips to more comprehensively reflect the urban environment as they can provide dynamic urban elements, such as crowd and traffic flow, whereas street view images can only reflect static conditions.

5. Conclusion

To contribute to building a more psychologically friendly urban environment, this study focuses on analyzing the impact of visual exposure on pedestrian psychological stress in a high-density context. Considering the long-term effects of the visual environment on physiological stress, we used the lagged visual exposure factors to build the regression models to demonstrate the relationship between SCL and the previous visual environments. There are several innovations in this study. First, it attempts to quantitatively understand the SCL responses to various visual elements in an outdoor urban environment. Second, this study determines the most influential lags of different visual exposure factors to better understand the effects of the visual environment, since SCL changes slowly over time and space according to different environmental stimuli. Besides, this study more adequately models the impact of the visual environment using spatial machine learning techniques and considers the spatial non-stationary.

The following conclusions can be drawn from the present study: 1. Our results are in line with the stress recovery theory that the trees in visual areas are helpful to relieve physiological stress. 2. The influential lags have wide ranges (from 40 m to 400 m), which is in line with the definition of SCL, where the visual impacts are lagged and the distances vary with different elements. The tree view factor has the smallest lag (80 m) and the objective proportion has the largest one (400 m) among all predictors. 3. The MLR models have an R^2 value of 0.466 and suggest that in a high-density environment, exposure to a larger tree view factor, sky proportion, and sign symbol view factor is associated with less psychological stress. Conversely, areas with the view of road view factor and object proportion incite more psychological stress. 4. The GRF model demonstrates a strong ability to predict pedestrian physiological stress and can explain 87.4% of the spatial variance of pedestrian psychological stress using only five visual exposure variables. The R^2 between the predicted SCL and the true values of the validation dataset is 0.869. 5. The proportion of sky, road, and trees has the largest impact on physiological stress. 6. The effects of the visual environment are spatially non-stationary, and the local models in commercial land use are stronger than those of residential land use.

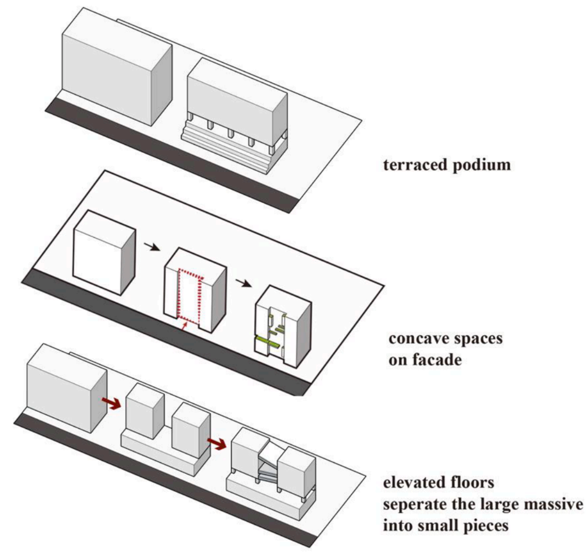

Fig. 12. An example to increase sky proportion.

This study confirms that the physiological stress can be effectively monitored with wearable sensors in outdoor built environments. It can provide urban planners, architects, and decision-makers with quantified and practicable reference to jointly foster good health and well-being, eventually contributing to a psychologically friendly future and sustainable urban environment for humans.

CRediT authorship contributor statement

M.C and L.X. contributed equally to this work and should be considered co-first authors.

Declaration of Competing Interest

The authors declare that they have no known competing financial interests or personal relationships that could have appeared to influence the work reported in this paper.

Data availability

The data that has been used is confidential.

Acknowledgments

The study is supported by a PGS studentship from The Chinese University of Hong Kong. It is also supported by the Fundamental Research Funds for the Central Universities (No. 2042023kf0004). The research gains ethics approval from The Chinese University of Hong Kong (Certificate No. S24601960).

Supplementary materials

Supplementary material associated with this article can be found, in the online version, at doi:10.1016/j.scs.2023.104695.

Reference

Alvarsson, J. J., Wiens, S., & Nilsson, M. E. (2010a). Stress recovery during exposure to nature sound and environmental noise. *International journal of environmental research and public health, 7*(3), 1036–1046. https://doi.org/10.3390/ijerph7031036

Alvarsson, J. J., Wiens, S., & Nilsson, M. E. (2010b). Stress recovery during exposure to nature sound and environmental noise. *International journal of environmental research and public health, 7*(3), 1036–1046.

Appleton, J. (1975). *The experience of landscape*. London: John Wiley and Sons.

Brady, T. F., Konkle, T., Alvarez, G. A., & Oliva, A. (2008). Visual long-term memory has a massive storage capacity for object details. *Proceedings of the National Academy of Sciences, 105*(38), 14325. https://doi.org/10.1073/pnas.0803390105

Brakus, J. J., Schmitt, B. H., & Zarantonello, L. (2009). Brand experience: What is it? How is it measured? Does it affect loyalty? *Journal of marketing, 73*(3), 52–68. %@ 0022-2429.

Breiman, L. (2001). Random Forests. *Machine Learning, 45*(1), 5–32. https://doi.org/10.1023/A:1010933404324

Brostow, G. J., Fauqueur, J., & Cipolla, R. (2009). Semantic object classes in video: A high-definition ground truth database. *Pattern Recognition Letters, 30*(2), 88–97. %@ 0167-8655.

Brunsdon, C., Fotheringham, S., & Charlton, M. (1998). Geographically weighted regression. *Journal of the Royal Statistical Society: Series D (The Statistician), 47*(3), 431–443.

Chatterjee, S. A., Daly, J. J., Porges, E. C., Fox, E. J., Rose, D. K., McGuirk, T. E., ..., et al. (2018). Mobility Function and Recovery After Stroke: Preliminary Insights From Sympathetic Nervous System Activity. *Journal of neurologic physical therapy : JNPT, 42*(4), 224–232. https://doi.org/10.1097/NPT.0000000000000238

Chen, L.-C., Zhu, Y., Papandreou, G., Schroff, F., & Adam, H. (2018). *Encoder-decoder with atrous separable convolution for semantic image segmentation.* Paper presented at the REAL CORP 2017.

Chung, L. C. H., Xie, J., & Ren, C. (2021). Improved machine-learning mapping of local climate zones in metropolitan areas using composite Earth observation data in Google Earth Engine. *Building and Environment, 199*, Article 107879.

Dawes, M. J., & Ostwald, M. J. (2014a). Prospect-Refuge theory and the textile-block houses of Frank Lloyd Wright: An analysis of spatio-visual characteristics using isovists. *Building and Environment, 80*, 228–240. https://doi.org/10.1016/j.buildenv.2014.05.026

Dawes, M. J., & Ostwald, M. J. (2014b). Testing the 'Wright Space': Using isovists to analyse prospect-refuge characteristics in Usonian architecture. *The Journal of Architecture, 19*(5), 645–666. https://doi.org/10.1080/13602365.2014.965722

Dawson, M., SCHELL, Anne M., & FILION, D. L (2001). The Electrodermal System. In J. T. Cacioppo, L. G. Tassinary, & G. B. Bernston (Eds.), *Handbook of psychophysiology* (2nd Ed). Cambridge: Cambridge Press.

De Silva, C. S., Warusavitharana, E. J., & Ratnayake, R. (2017). An examination of the temporal effects of environmental cues on pedestrians' feelings of safety. *Computers, Environment and Urban Systems, 64*, 266–274. https://doi.org/10.1016/j.compenvurbsys.2017.03.006

Department, P. (2015). Hong Kong planning standards and guidelines. *Urban Design Guidelines*.

Dosen, A. S., & Ostwald, M. J. (2016). Evidence for prospect-refuge theory: A meta-analysis of the findings of environmental preference research. *City, territory and architecture, 3*(1), 1–14.

Fisher-Gewirtzman, D., Burt, M., & Tzamir, Y. (2003). A 3-D Visual Method for Comparative Evaluation of Dense Built-up Environments. *Environment and Planning B: Planning and Design, 30*(4), 575–587. https://doi.org/10.1068/b2941

Fisher-Gewirtzman, D., & Wagner, I. A. (2003). Spatial Openness as a Practical Metric for Evaluating Built-up Environments. *Environment and Planning B: Planning and Design, 30*(1), 37–49. https://doi.org/10.1068/b12861

Fotheringham, A. S., Brunsdon, C., & Charlton, M. (2003). *Geographically weighted regression: The analysis of spatially varying relationships*. John Wiley & Sons.

Gatti, E., Calzolari, E., Maggioni, E., & Obrist, M. (2018). Emotional ratings and skin conductance response to visual, auditory and haptic stimuli. *Scientific data, 5*, Article 180120. https://doi.org/10.1038/sdata.2018.120

Georganos, S., Grippa, T., Vanhuysse, S., Lennert, M., Shimoni, M., Kalogirou, S., et al. (2018). Less is more: Optimizing classification performance through feature selection in a very-high-resolution remote sensing object-based urban application. *GIScience & remote sensing, 55*(2), 221–242.

Griego, D., Buff, V., Hayoz, E., Moise, I., & Pournaras, E. (2017). *Sensing and Mining Urban Qualities in Smart Cities*. Paper presented at the IEEE 31st.

Grover, S., Sahoo, S., Mehra, A., Avasthi, A., Tripathi, A., Subramanyan, A., ..., et al. (2020). Psychological impact of COVID-19 lockdown: An online survey from India. *Indian journal of psychiatry, 62*(4), 354–362.

Hijazi, I. H., Koenig, R., Schneider, S., Li, X., Bielik, M., Schmit, G. N. J., et al. (2016). Geostatistical Analysis for the Study of Relationships between the Emotional Responses of Urban Walkers to Urban Spaces. *International Journal of E-Planning Research, 5*(1), 1–19. https://doi.org/10.4018/ijepr.2016010101

Huang, Q., Yang, M., Jane, H.-a., Li, S., & Bauer, N. (2020). Trees, grass, or concrete? The effects of different types of environments on stress reduction. *Landscape and Urban Planning*, 193. https://doi.org/10.1016/j.landurbplan.2019.103654

Javadi, A. H., Emo, B., Howard, L. R., Zisch, F. E., Yu, Y., Knight, R., ..., et al. (2017). Hippocampal and prefrontal processing of network topology to simulate the future. *Nature Commun, 8*, 14652. https://doi.org/10.1038/ncomms14652

Kalat, J. W. (2015). *Biological psychology*. Cengage Learning.

Kalogirou, S. (2016). Destination Choice of Athenians: An Application of Geographically Weighted Versions of Standard and Zero Inflated Poisson Spatial Interaction Models. *Geographical Analysis, 48*(2), 191–230. https://doi.org/10.1111/gean.12092

Kaplan, R., & Kaplan, S. (1989). *The experience of nature: A psychological perspective*. CUP Archive.

Kim, J., Yadav, M., Chaspari, T., & Ahn, C. R. (2020). Saliency detection analysis of collective physiological responses of pedestrians to evaluate neighborhood built environments. *Advanced Engineering Informatics, 43*, Article 101035. https://doi.org/10.1016/j.aei.2020.101035

Knöll, M., Neuheuser, K., Cleff, T., & Rudolph-Cleff, A. (2017). A tool to predict perceived urban stress in open public spaces. *Environment and Planning B: Urban Analytics and City Science.* , Article 026581351668697. https://doi.org/10.1177/0265813516686971

Davis, Larry S., & L Benedikt, M (1979). Computational Models of Space Isovists and Isovist Fields. *Computer Graphic and Image Procssing*, 11.

Lederbogen, F., Kirsch, P., Haddad, L., Streit, F., Tost, H., Schuch, P., ..., et al. (2011). City living and urban upbringing affect neural social stress processing in humans. *Nature, 474*(7352), 498–501. https://doi.org/10.1038/nature10190

Li, X., Hijazi, I., Koenig, R., Lv, Z., Zhong, C., & Schmitt, G. (2016). Assessing Essential Qualities of Urban Space with Emotional and Visual Data Based on GIS Technique. *ISPRS International Journal of Geo-Information, 5*(11), 218. https://doi.org/10.3390/ijgi5110218

Li, Y., Li, Z.-L., Wu, H., Zhou, C., Liu, X., Leng, P., ..., et al. (2023). Biophysical impacts of earth greening can substantially mitigate regional land surface temperature warming. *NATURE COMMUNICATIONS, 14*(1), 121. https://doi.org/10.1038/s41467-023-35799-4

Lin, F.-C., She, S.-J., Ngo, H.-H., Dow, C.-R., & Hsu, F.-R. (2021). A wearable embedded system for assisting cognition of visually impaired people by street scene description. *Journal of Computers (Taiwan), 32*(1), 102–119.

Lin, W., Chen, Q., Jiang, M., Tao, J., Liu, Z., Zhang, X., ..., et al. (2020). Sitting or Walking? Analyzing the Neural Emotional Indicators of Urban Green Space Behavior with Mobile EEG. *Journal of Urban Health, 97*(2), 191–203. https://doi.org/10.1007/s11524-019-00407-8

Lindal, P. J., & Hartig, T. (2013). Architectural variation, building height, and the restorative quality of urban residential streetscapes. *Journal of Environmental Psychology, 33*, 26–36. https://doi.org/10.1016/j.jenvp.2012.09.003

Mangone, G., Capaldi, C. A., van Allen, Z. M., & Luscuere, P. G. (2017). Bringing nature to work: Preferences and perceptions of constructed indoor and natural outdoor workspaces. *Urban Forestry & Urban Greening, 23*, 1–12. https://doi.org/10.1016/j.ufug.2017.02.009

Marianne, H.M., & Knöll, M. (2017). *The relationship between visual fields and perceived stress in a public*. Paper presented at the 11th International Space Syntax Symposium, Lisbon.

Mavros, P., Austwick, M. Z., & Smith, A. H. (2016). Geo-EEG: Towards the Use of EEG in the Study of Urban Behaviour. *Applied Spatial Analysis and Policy, 9*(2), 191–212. https://doi.org/10.1007/s12061-015-9181-z

Mavros, P., J Wälti, M., Nazemi, M., Ong, C. H., & Hölscher, C (2022). A mobile EEG study on the psychophysiological effects of walking and crowding in indoor and outdoor urban environments. *Nature, 12*(1), 18476. https://doi.org/10.1038/s41598-022-20649-y

Mazumder, R., Spiers, H. J., & Ellard, C. G. (2022). Exposure to high-rise buildings negatively influences affect: Evidence from real world and 360-degree video. *Cities & Health, 6*(6), 1081–1093. https://doi.org/10.1080/23748834.2020.1839302

Millar, G. C., Mitas, O., Boode, W., Hoeke, L., de Kruijf, J., Petrasova, A., et al. (2021). Space-time analytics of human physiology for urban planning. *Computers, Environment and Urban Systems*, 85. https://doi.org/10.1016/j.compenvurbsys.2020.101554

Mir, M., Nasirzadeh, F., Bereznicki, H., Enticott, P., Lee, S., & Mills, A. (2023). Construction noise effects on human health: Evidence from physiological measures. *Sustainable Cities and Society, 91*, Article 104470. https://doi.org/10.1016/j.scs.2023.104470

Neale, C., Aspinall, P., Roe, J., Tilley, S., Mavros, P., Cinderby, S., ..., et al. (2020). The impact of walking in different urban environments on brain activity in older people. *Cities & Health, 4*(1), 94–106. https://doi.org/10.1080/23748834.2019.1619893

Nold, C. (2009). *EmotionalCartography: Technologies of the self*.

Ren, C., Cai, M., Li, X., Shi, Y., & See, L. (2020). Developing a rapid method for 3-dimensional urban morphology extraction using open-source data. *Sustainable Cities and Society, 53*, Article 101962. %@ 102210-106707.

Ulrich, Roger S., Simons, Robert F., Losito, Barbara D., Fiorito, Evelyn, Mile, Mark A., & Zelson, M. (1991). Stress recovery during exposure to natural and urban environments. *Journal of Environmental Psychology, 11*.

Rogerson, M., Gladwell, V. F., Gallagher, D. J., & Barton, J. L. (2016). Influences of Green Outdoors versus Indoors Environmental Settings on Psychological and Social Outcomes of Controlled Exercise. *International journal of environmental research and public health, 13*(4). https://doi.org/10.3390/ijerph13040363

Saladino, V., Algeri, D., & Auriemma, V. (2020). The psychological and social impact of Covid-19: New perspectives of well-being. *Frontiers in psychology*, 2550.

Serafini, G., Parmigiani, B., Amerio, A., Aguglia, A., Sher, L., & Amore, M. (2020). The psychological impact of COVID-19 on the mental health in the general population. *QJM: An International Journal of Medicine, 113*(8), 531–537. https://doi.org/10.1093/qjmed/hcaa201

Shi, Y., Ren, C., Lau, K. K.-L., & Ng, E. (2019). Investigating the influence of urban land use and landscape pattern on PM2.5 spatial variation using mobile monitoring and WUDAPT. *Landscape and Urban Planning, 189*, 15–26. https://doi.org/10.1016/j.landurbplan.2019.04.004

Kaplan, Stephen (1983). A model of person-environment compatibility. *Environment and Behavior, 15*(3), 22.
The Mental Health Association of Hong Kong. (2016). *Hong Kong Mental Morbidity Survey* Retrieved from.
The World Bank. (2018). Population density (people per sq. km of land area) - Hong Kong SAR, China. Retrieved from https://data.worldbank.org/indicator/EN.POP.DNST?locations=HK.
The Mental Health Association of Hong Kong. (2020). *Territory-wide Mental Health Index Index Survey 2020*.
Turner, A., Doxa, M., O'Sullivan, D., & Penn, A. (2001). From Isovists to Visibility Graphs: A Methodology for the Analysis of Architectural Space. *Environment and Planning B: Planning and Design, 28*(1), 103–121. https://doi.org/10.1068/b2684
Weich, S. (2002). Mental health and the built environment: Cross-sectional survey of individual and contextual risk factors for depression. *The British Journal of Psychiatry, 180*(5), 428–433. https://doi.org/10.1192/bjp.180.5.428
Winz, M., Söderström, O., Rizzotti-Kaddouri, A., Visinand, S., Ourednik, A., Küster, J., et al. (2022). Stress and emotional arousal in urban environments: A biosocial study with persons having experienced a first-episode of psychosis and persons at risk. *Health & place, 75*, Article 102762. https://doi.org/10.1016/j.healthplace.2022.102762
World Health Organization. (2022). *World mental health report: Transforming mental health for all*. Retrieved from.
Xiang, L., Cai, M., Ren, C., & Ng, E. (2021). Modeling pedestrian emotion in high-density cities using visual exposure and machine learning: Tracking real-time physiology and psychology in Hong Kong. *Building and Environment, 205*, Article 108273. https://doi.org/10.1016/j.buildenv.2021.108273
Yin, J., Zhu, S., MacNaughton, P., Allen, J. G., & Spengler, J. D. (2018). Physiological and cognitive performance of exposure to biophilic indoor environment. *Building and Environment, 132*, 255–262. https://doi.org/10.1016/j.buildenv.2018.01.006
Yu, R., Gu, N., & Ostwald, M. (2016). The mathematics of spatial transparency and mystery: Using syntactical data to visualise and analyse the properties of the Yuyuan Garden. *Visualization in Engineering, 4*(1). https://doi.org/10.1186/s40327-016-0033-y
Zheng Chen, Sebastian Schulz, Xiaofan He, & Yifan Chen. (2016). A Pilot Experiment on Affective Multiple Biosensory Mapping for Possible Application to Visual Resource Analysis and Smart Urban Landscape Design. Paper presented at the REAL CORP 2016.